Proceedings of the ASME 2023
50th Annual Review of Progress in
Quantitative Nondestructive Evaluation
QNDE2023
July 24-27, 2023, Austin, Texas

QNDE2023-118316

SELF-SENSING PIEZOELECTRIC COMPOSITE STRUCTURES USING DISPERSE ELECTRO-MECHANICAL IMPEDANCE MEASUREMENTS

Shulong Zhou
University of Michigan-Shanghai Jiao Tong University Joint Institute, Shanghai Jiao Tong University, Shanghai, China

Yanfeng Shen
University of Michigan-Shanghai Jiao Tong University Joint Institute, Shanghai Jiao Tong University, Shanghai, China

Yuan Tian
Wuxi city huifeng electronic coltd, Jiangsu, China

Bao Wang
Wuxi city huifeng electronic coltd, Jiangsu, China

Chunquan Wang
Wuxi city huifeng electronic coltd, Jiangsu, China

ABSTRACT

This paper proposes a novel family of intelligent piezoelectric composite structures for the purpose of establishing structural self-awareness via disperse measurements of Electro-mechanical Impedance Spectroscopy (EMIS) methodology. The target of the current study aims at developing a functional composite material that embraces both load bearing and self-sensing capabilities at the same time. This is achieved by incorporating active material components, such as piezoelectric ingredients, in the structural component, forming a disperse and dense sensing grid, combined with active sensing methodologies. To develop a deep insight into the mechanism of the intelligent structure, coupled-field finite element models are constructed for verifying the feasibility of the EMIS for damage detection. In particular, the model employs the Equivalent Average Parameter (EAP) method, utilizing overall and nominal parameters, in order to simulate the self-sensing composites. A Root Mean Square Deviation (RMSD) damage metric is subsequently applied to determine the position of the structural damage. Furthermore, the manufacturing process of a piezoelectric composite beam structure is introduced in detail. meticulously crafted through a continuous process of material ratio optimization and process step refinement. Careful manufacturing parameters are explored to ensure the highest extent of sensitivity and reliability. Finally, experimental validation of the EMIS method is performed, showcasing the feasibility and accuracy of the impedance spectra for the damage location and quantification. The paper finished with summary, concluding remarks, and suggestions for future work.

Keywords: electromechanical impedance spectroscopy; piezoelectricity; self-awareness; smart structures; active sensing

1. INTRODUCTION

Structural Health Monitoring (SHM) aims at developing real-time interrogation methodologies for evaluating structural integrity and detecting potential hazards of structural damage. The advent of smart structures equipped with self-sensing capabilities represents a promising breakthrough in the field of structural engineering. These structures possess the ability to monitor their own condition, a feature that has the potential to drastically reduce maintenance expenses and prevent catastrophic failures, rendering them particularly valuable characteristics for constructing safer and more intelligent infrastructures. The integration of self-sensing capabilities into load-bearing structures has the potential to substantially enhance this facet of infrastructure management [1].

Piezoelectric materials have garnered significant attention as actuation and sensing devices in applications pertaining to structural health monitoring and nondestructive evaluation. In particular, Piezoelectric Wafer Active Sensors (PWAS) have emerged as a viable solution for crack detection. These sensors are usually bounded to the surfaces of host structures, thereby facilitating reliable and non-invasive monitoring of structural integrity [2]. The surface-bonding approach has a weakness in that sensors attached in this way can become debonded and peeled off, and are vulnerable to scratches. Furthermore, these sensors are brittle and stiff due to their constituent materials and processing. On the other hand, composite materials are excellent options for load-bearing components in mechanical and

aerospace designs due to their exceptional properties. Minakuchi and Takeda implemented fiber optic sensors in aerospace composite structures and introduced two new technical concepts the "smart crack arrester" and "hierarchical sensing system" to detect impact damage [3]. Their research marched a significant step forward in integrating advanced sensing technologies in aerospace systems. Krishnamurthy et al. successfully detected delamination by incorporating magnetostrictive particle layers within composite laminates [4]. Nonetheless, the embedding of magnetostrictive particles within the laminates unavoidably creates stress concentrations, thereby causing the formation of local cracks over time. To mitigate these effects, researchers have explored an alternate strategy of modifying material properties through the incorporation of functional components. Tallman et al. adopted nanocomposites using carbon nanofiber and polyurethane, which resulted in enhanced delamination detection and distributed strain sensing [5]. Haghiashtiani and Greminger employed polyvinylidene fluoride (PVDF) as a composite matrix for integrated structural load sensing [6]. Liu et al. fabricated PVDF-TrFE transducers to measure defects in multilayer bonded structures using the ZGV waves [7]. Li et al. developed a coated sensor network made of carbon nanotubes (CNTs) to spray and be deposited onto the surface of complex structures [8]. In the interim, the implementation of these innovative techniques has brought to light certain limitations, namely a reduced actuation capacity and increased expenses. Consequently, there is a constantly developing need for novel structure-sensor integration systems that potentiates to herald a new era of self-sensing intelligent structures.

Electro-mechanical Impedance Spectroscopy (EMIS) has been widely investigated as an effective technique for structural health monitoring and nondestructive evaluation. It utilizes PWAS to monitor the health of a structure non-destructively by measuring the electrical impedance at the sensors' terminals, which reflects changes in the material properties caused by damage like debonding, delamination, void, crack, creep, etc. Considerable resources and efforts have been invested in implementing the EMIS technique for various SHM applications, demonstrating its effectiveness across a wide range of engineering domains. Using the electromechanical impedance technique, Giurgiutiu and Zagrai performed damage detection on aging aircraft panels [9]. Gresil et al. demonstrated the capability of EMIS in monitoring aerospace composite materials [10]. Soh et al. utilized PWAS transducers to perform localized monitoring of civil infrastructures [11]. Kim et al. and Divsholi and Yang developed EMIS applications for monitoring concrete structures [12, 13]. Park et al., Na, and Raju et al. demonstrated the effectiveness of EMIS for inspecting pipeline systems [14, 16]. Further applications of the EMIS technique are discussed in review articles authored by Farrar and Inman as well as Annamdas and Soh [17, 18].

This paper presents a new type of intelligent piezoelectric composite structures that utilized EMIS to establish structural self-awareness. Finite element models are used to understand the mechanism of EMIS for damage detection. The models are based on the Equivalent Average Parameter (EAP) method. The fabrication process is developed to ensure the highest degree of sensitivity and reliability and elaborated for experimental demonstration. Finally, the accuracy of the EMIS method is experimentally validated by testing impedance spectra for case studies.

2. NUMERICAL MODELING OF PIEZOELECTRIC COMPOSITES FOR ESTABLISHING STRUCTURAL SELF-AWARENESS

In this section, the Finite Element Model (FEM) of the proposed piezoelectric composite is presented with its fundamental parameters. Subsequently, delving into an exploration of the intrinsic EMIS of a piezoelectric composite beam, various case studies are investigated to scrutinize the effect of EMIS for diagnosing structural damage.

2.1 Parameterization of the piezoelectric composite

FIGURE 1 illustrates a schematic of the piezoelectric composite material. It is comprised of resin evenly mixed with piezoelectric ceramic powder. It was noteworthy that the material of the current research was composed of PZT-powder-enriched epoxy. Electrodes could be arranged at any desired location, and once these electrodes were poled, the printed electrode pairs would inherit the piezoelectric property, forming a disperse and dense active sensor array. Consequently, this piezoelectric component was endowed with both actuation and sensing capabilities. Furthermore, the electrode could be designed to impart a "neuron" to any location, thereby providing a perceptual effect wherever it was needed.

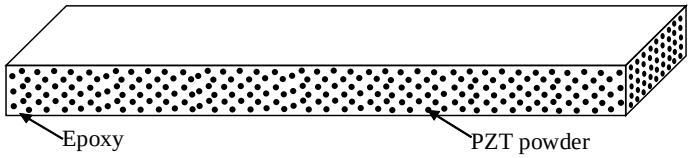

FIGURE 1: SCHEMATIC OF THE PIEZOELECTRIC COMPOSITE STRUCTURAL CONSTITUENT

In this paper, the model employed the EAP method for simulating the piezoelectric and load-bearing performance. Among which, the piezoelectric composite stiffness matrix was extracted by scaling an equivalent PZT material stiffness matrix:

$$\left[C_p\right]=\begin{bmatrix} 21 & 10.61 & 10.61 & 0 & 0 & 0 \\ 10.61 & 21 & 10.61 & 0 & 0 & 0 \\ 10.61 & 10.61 & 18.18 & 0 & 0 & 0 \\ 0 & 0 & 0 & 5.195 & 0 & 0 \\ 0 & 0 & 0 & 0 & 4.76 & 0 \\ 0 & 0 & 0 & 0 & 0 & 4.76 \end{bmatrix} \text{GPa} \qquad (1)$$

The piezoelectric coefficient is turned down owing to a scattered and lower powder ratio in the piezoelectric composite, compared with the existing piezoelectric ceramic actuators:

$$\left[e_p\right]=\begin{bmatrix} 0 & 0 & -4.01 \\ 0 & 0 & -4.01 \\ 0 & 0 & 9.16 \\ 0 & 0 & 0 \\ 0 & 6.42 & 0 \\ 6.42 & 0 & 0 \end{bmatrix} \text{C/m}^2 \quad (2)$$

The density of the piezoelectric composite material is assumed to be 1960 kg/m^3 and the dielectric matrix is kept the same as the PZT materials:

$$\left[\varepsilon_p\right]=\begin{bmatrix} 4.3 & 0 & 0 \\ 0 & 4.3 & 0 \\ 0 & 0 & 4.3 \end{bmatrix} \quad (3)$$

2.2 FEM of a piezoelectric composite beam

The three-dimensional FEMs displayed in FIGURE 2 are employed to simulate the EMIS active sensing procedure. To numerically demonstrate the EMIS characteristics, a piezoelectric composite beam measuring 100 mm in length, 10 mm in width, and 2 mm in thickness was specifically designed to enable the investigation of local damage effects on the impedance response. The sensing neurons were created by implementing polarized electrodes, which were circular in shape with a diameter of 6 mm. These electrodes were positioned at a distance of 10 mm from one another, with a total of ten pairs of sensing electrodes designed to monitor the occurrence of local damage.

The overall damage configurations are displayed in FIGURE 2b and 2c, showing the placement of the simulated structural damage. To simulate the structural damage, the local material stiffness was decreased between electrode core #3 and electrode core #4, as well as between electrode core #9 and electrode core #10 for the second damaged case. These damage configurations were then utilized to evaluate their influence on the EMIS characteristics. After obtaining the local electromechanical impedance spectrum for each electrode for the pristine case, the spectra were used as the reference signals. Any subsequent damage near a specific electrode would result in corresponding changes in the impedance spectra of the sensing locations, which could be utilized to identify the approximate location of the damage.

A coupled-field harmonic analysis was performed by sweeping the frequency from 20 kHz to 420 kHz in a meticulous manner consisting of 1200 steps. The entire set of positive electrodes, portrayed in Figure 2, were connected and subjected to a unit voltage, while the negative counterparts positioned on the opposite side were grounded, and their electric potential were set to 0. To ensure a precise evaluation of the transducer's electro-mechanical impedance, the structural modal damping ratio was set at 0.002. The electric charges at the electrodes were then extracted with respect to frequency, thereby providing a comprehensive understanding of the sensing elements' performance characteristics across a wide range of electrical and mechanical scenarios.

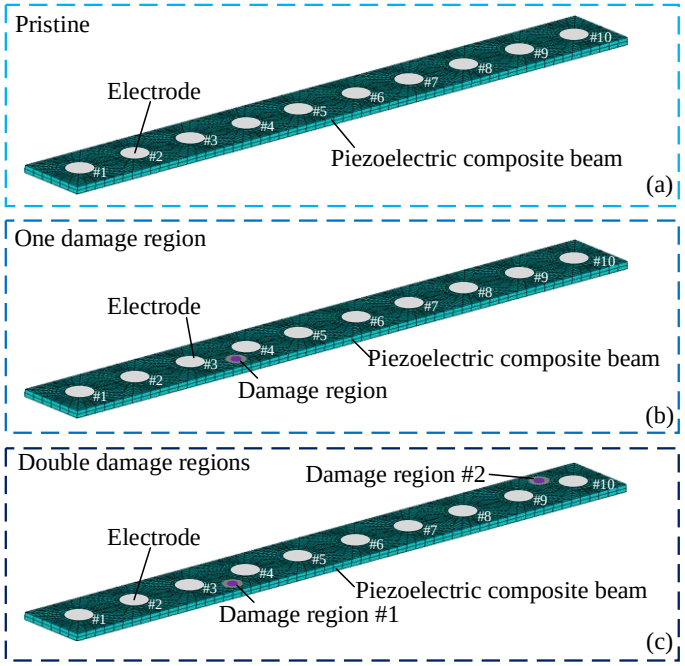

FIGURE 2: FEMS FOR EMIS ACTIVE SENSING OF A PIEZOELECTRIC COMPOSITE BEAM: (A) PRISTINE CASE; (B) ONE DAMAGE REGION CASE; (C) DOUBLE DAMAGE REGIONS CASE

2.3 Simulation results of EMIS active sensing

For demonstrating the simulation results, FIGURE 3a presents the EMIS curves at sensing location #3 as well as the corresponding structural resonance patterns at the peak response (208.6 kHz). The impedance spectrum was obtained from electrode pair #3, located proximal to the first simulated damage. When compared to the undamaged scenario, the majority of electromechanical impedance peaks displayed a reduction in amplitude and a shift in position upon damage occurrence, with the most discernible peak being observed.

FIGURE 3b depicts the resonance response of the vibrating, beam for both pristine and damaged states. In the pristine case, the symmetric resonance pattern was observed throughout the entire structure, with the primary vibrating energy localized in the vicinity of the excited electrode region. It was evident that the resonance energy was locally concentrated around the active electrode, providing an approximate and localized sensitive feature for the impedance spectrum. However, when the damage was located nearby the excited electrode, the equivalent stress distribution was thoroughly disrupted, with the high-stress region being concentrated surrounding the damage. Simultaneously, it was observed that damage situated far away from the excitation electrode had negligible impact on the stress distribution, as also indicated by the EMI data. Therefore, the existence of damage altered the resonance frequency of the structure, leading to a complete modification of the stress distribution. Furthermore, the local sensitivity of EMIS method

provides the possibility of precise damage location estimation via a disperse and dense sensing array.

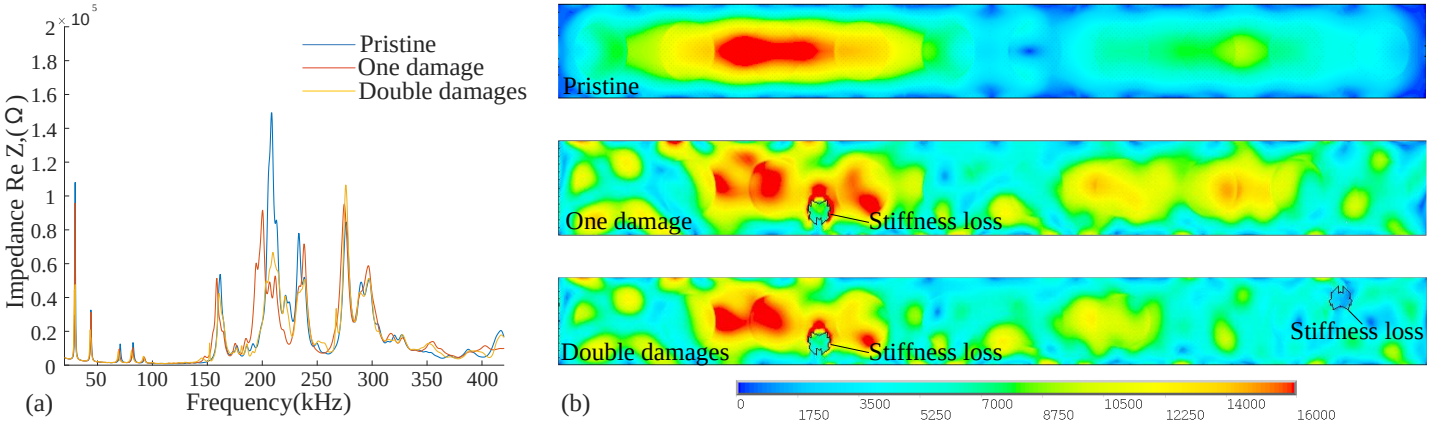

FIGURE 3: (A) REAL PART OF ELECTRO-MECHANICAL IMPEDANCE SPECTRUM OF THE PIEZOELECTRIC COMPOSITE BEAM; (B) SNAPSHOTS OF THE STRUCTURAL RESONANCE AT 208.6 KHZ

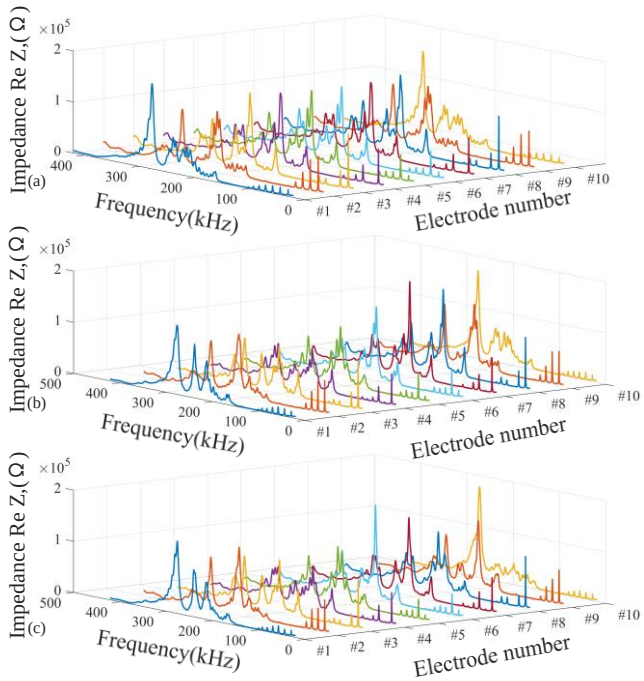

FIGURE 4: ELECTRO-MECHANICAL IMPEDANCE SPECTRA OF THE BEAMS AT DIFFERENT ELECTRODE PAIRS: (A) PRISTINE CASE; (B) ONE DAMAGE REGION CASE; (C) DOUBLE DAMAGE REGIONS CASE

The presented results in FIGURE 4 illustrate the electro-mechanical impedance spectra at each electrode pairs for all the pristine and damage cases. Notably, the electromechanical impedance spectrum exhibited symmetry along the central axis for the pristine structure. By scrutinizing the EMI spectra of all electrodes in three different cases, it became evident that any damage incurred would only affect the spectra of the electrodes very close to it, while the influence was negligible for the electrodes situated far away. Of particular interest was electrode #10, wherein the added damage in one damage case did not significantly alter the spectrum compared to the undamaged state, likely due to the considerable distance between the damage and the electrode. These results were in line with the stress nephogram analysis findings in FIGURE 3b. To sum, the electromechanical impedance method focused primarily on the change of local materials and properties.

2.4 RMSD metric for damage quantification

The selection of the appropriate range of the sweeping frequency band can wield considerable influence on the efficacy of the damage detection methodology employing the electromechanical impedance technique [19]. In order to compare the impedance spectra of the undamaged and damaged cases, this research employed the root mean square deviation (RMSD) damage metric, defined as follows:

$$RMSD = \sqrt{\sum_{i=1}^{n}[\mathrm{Re}(Z_i) - \mathrm{Re}(Z_i^0)]^2 / \sum_{i=1}^{n}\mathrm{Re}(Z_i^0)^2} \quad (4)$$

where N represents the quantity of frequency points present in the spectrum, while the superscript 0 denotes the pristine and unaltered state of the structure, and Z stands for the impedance measurement at the corresponding frequency.

RMSD is primarily used to quantify the similarity between two structures. It provides a measure of the average deviation between the corresponding impedance in two structures. The value of RMSD is normalized by the maximum RMSD value among all the cases in FIGURE 5, the RMSD value was utilized as an indicator of the algorithm's accuracy. The algorithm adeptly captured the impedance discrepancy between the pristine and damaged cases. The electrode situated close to the site of damage displayed a substantial increase in the RMSD value. With the presence of two damage locations, the identification of two distinct peaks of RMSD can be clearly observed. The

numerical results indicate the proposed piezoelectric composite structure can successfully execute the EMI technique for the purpose of establishing structural self-awareness.

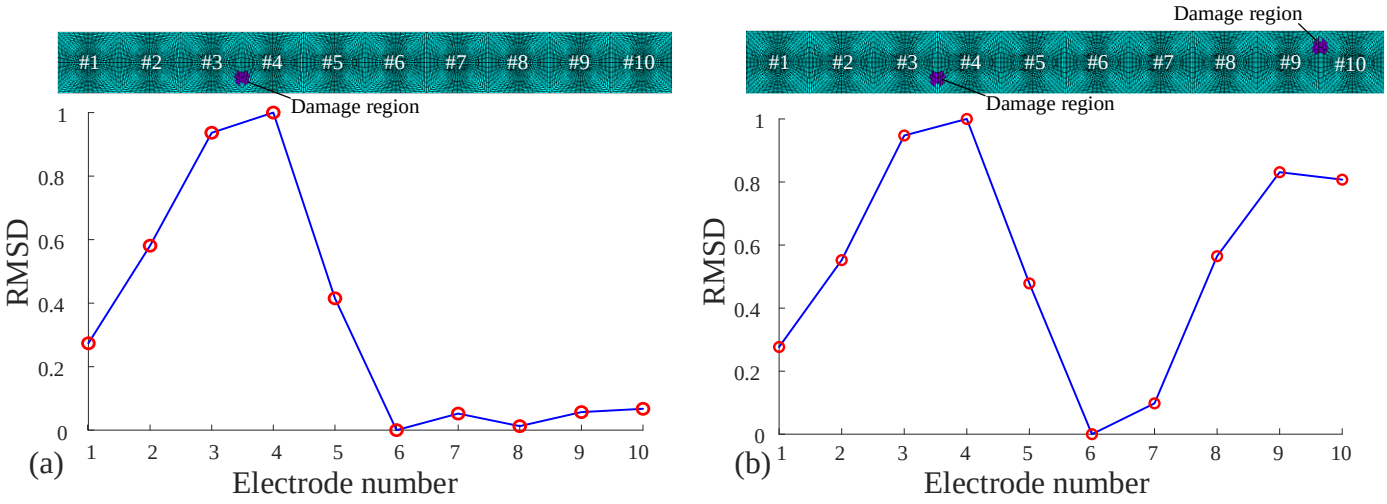

FIGURE 5: RMSD FOR THE DAMAGE CASES: (A) ONE DAMAGE REGION CASE; (B) TWO DAMAGE REGIONS CASE

3. FABRICATION OF PIEZOELECTRIC COMPOSITE TEST SPECIMEN

The piezoelectric composite structure was fabricated by mixing PZT powder and epoxy resin at a weight ratio of 5:1. The epoxy resin was a product of Wuxi City Huifeng Electronic Co., Ltd, consisting of resin (HF-005) and hardener (HF-006). The preparation involved a meticulous approach, where the mixture was sonicated for dispersion using vacuum-based equipment, poured into a specific mold, and subjected to a vacuum device for extracting any bubbles during curing. The curing temperature was maintained at 60 degrees Celsius for 4 hours. In order to obtain a polarized piezoelectric composite structure, the poling electrodes were coated with silver screen printing at 110 degrees Celsius for 45 min. Poling was performed under 60 kV/mm for 15 min, utilizing a high-voltage amplifier, submerged in oil. To ensure complete polarization, special attention was given to the initial polarization electrode's coverage of the entire upper and lower surface of the piezoelectric composite structure. Subsequently, the sample was machined to meet precise dimensional requirements, and the excess silver layer was removed from the surface of the structure through laser carving, retaining the necessary electrode parts. Moreover, the tailored piezoelectric composite structure distinguishes itself from existing PZT actuators by eliminating the complex assembly procedures associated with piezoelectric wafers, such as sintering under high-temperature environments during fabrication. FIGURE 6 depicts the manufacturing process of the piezoelectric composite structure, demonstrating the meticulous approach employed to fabricate a highly polarized, precisely dimensioned piezoelectric composite beam.

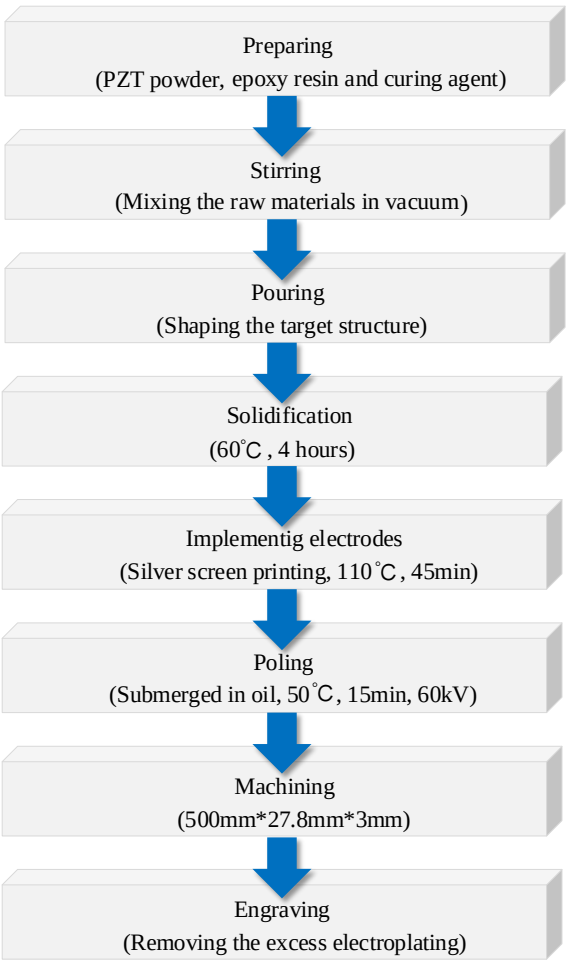

FIGURE 6: FLOW CHART OF MANUFACTURING PROCEDURE FOR THE PIEZOELECTRIC COMPOSITE STRUCTURE

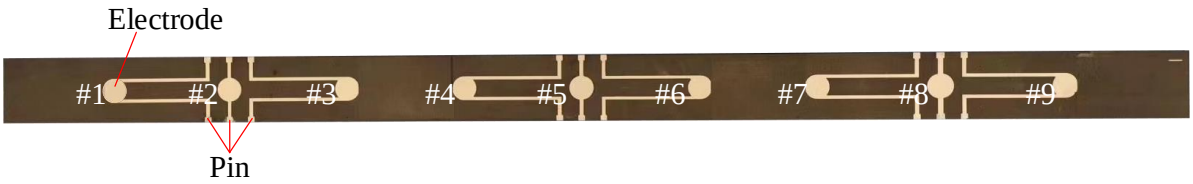

FIGURE 7: PIEZOELECTRIC COMPOSITE BEAM SPECIMEN FOR EXPERIENTAL TESTS

FIGURE 7 illustrates the beam specimen fabricated by the piezoelectric composite. A beam measuring 500 millimeters in length, 27.8 mm in width, and 3 mm in thickness was produced for experimental testing. To facilitate subsequent electrode voltage loading, nine pairs of electrodes measuring 10 mm in diameter were strategically positioned on both the upper and lower surfaces of the beam, with a distance of 50 mm between each pair. Notably, to enable the desired electrode voltage loading, a portion of the silver layer was retained to form a conductive connector. The implementation of these connectors engendered the reliability of the interface, as it allowed for the utilization of convenient and gentle connection, in case of any unforeseen damage or failure, thereby ameliorating its resilience and practicality.

4. EXPERIMENTAL DEMONSTRATION OF EMIS FOR ESTABLISHING SELF-AWRENESS OF PIEZOELECTRIC COMPOSITE STRUCTURES

In this section, a systematic series of experiments was conducted to assess the efficacy of EMIS for creating self-awareness in piezoelectric composite structures. FIGURE 8 illustrates the experimental setup employed in the study. To assess local structural damage, an iron block was affixed to the sample's surface to mimic a damage via altering the local stiffness and resonance of the structure. At each end of the specimen, sponge blocks were positioned while the crocodile clamp was attached at the designated connectors to establish a detachable connection. Electro-mechanical impedance data at the electrodes were obtained using the Bode 100 impedance analyzer manufactured by OMICRON LAB. In line with the approach taken in the numerical simulation, a comparative assessment was performed by means of frequency sweeping using the impedance analyzer to exhibit resonance in both pristine and damaged conditions. The impedance spectra obtained from experimental measurements are depicted in FIGURE 9. It was noteworthy that the impedance spectrum obtained from the experiment showed discrepancies from the numerical results due to the higher overall damping of the material in the actual manufactured specimen. When considering the frequencies within the range of 20 kHz to 90 kHz, in the impedance curve of the damage case, numerous electromechanical resonance peaks were detected. Nevertheless, the electrode under scrutiny in the original investigation exhibited no discernible formants, and the impedance spectrum was notably extensive. The presence of distinctive regional variations creates conditions for the detection and localization of damage sites.

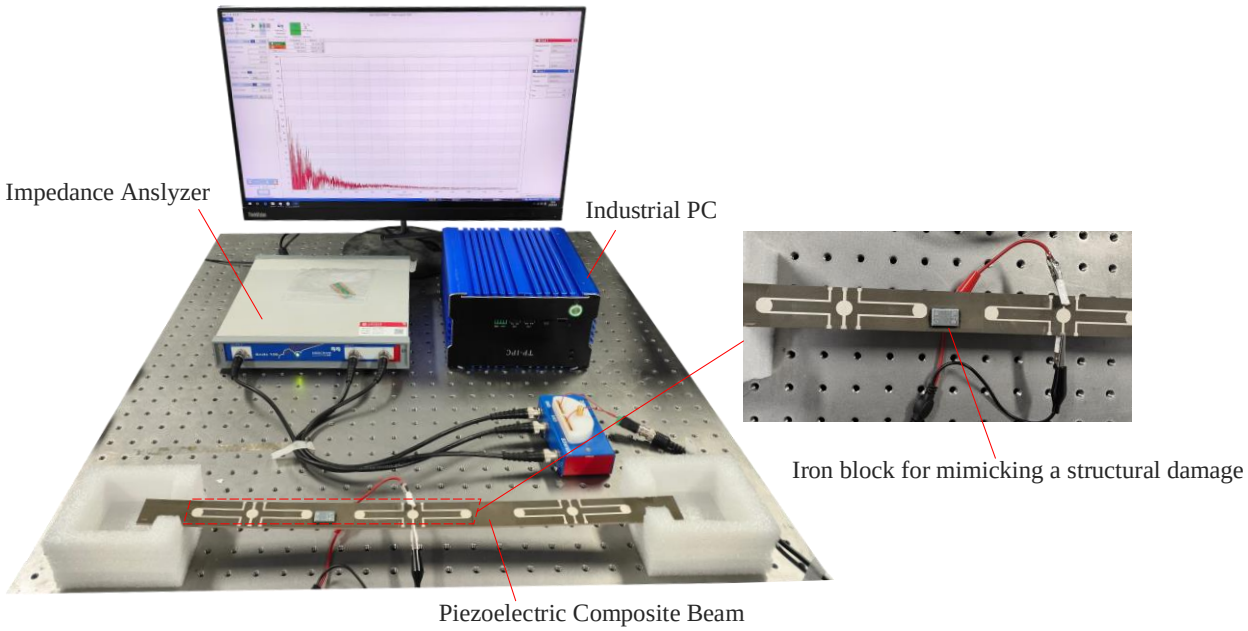

FIGURE 8: THE OVERALL EXPERIMENTAL SETUP

The RMSD algorithm evinced exceptional aptitude in detecting the impedance discrepancy between the pristine and the damaged scenarios, as is evident from FIGURE 10. The electrode situated close to the damage site exhibited a considerable increase in the RMSD value. Of particular significance is the observation that electrode #3, situated in the immediate vicinity of the damage site, elicited the most substantial resonance variation. However, it was noteworthy that the extent of damage coverage was smaller than the predictive simulation.

The results of this experiment provided persuasive validation and demonstration that the proposed piezoelectric composites could effectively employ the electro-mechanical impedance technique for the purpose of establishing its self-awareness as a smart structural component.

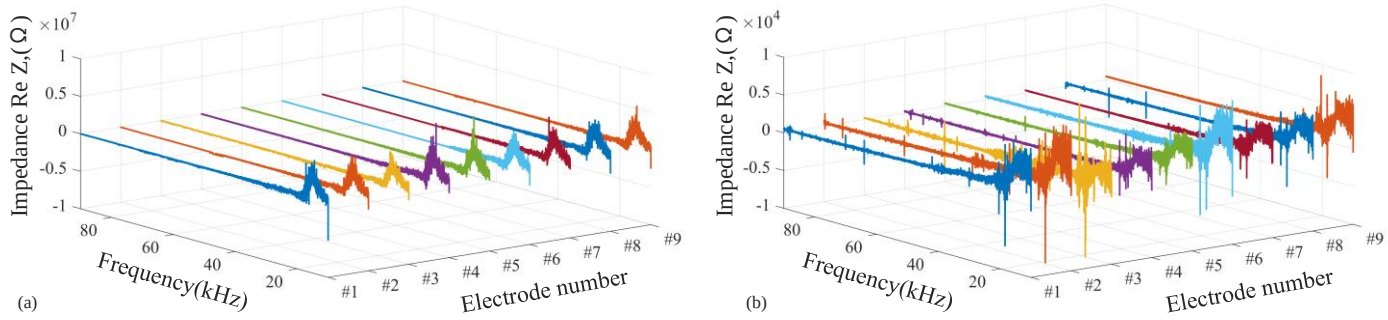

FIGURE 9: EXPERIMENTAL IMPEDANCE SPECTRA COMPARISON BETWEEN A) THE PRISTINE CASE AND B) THE DAMAGED CASE

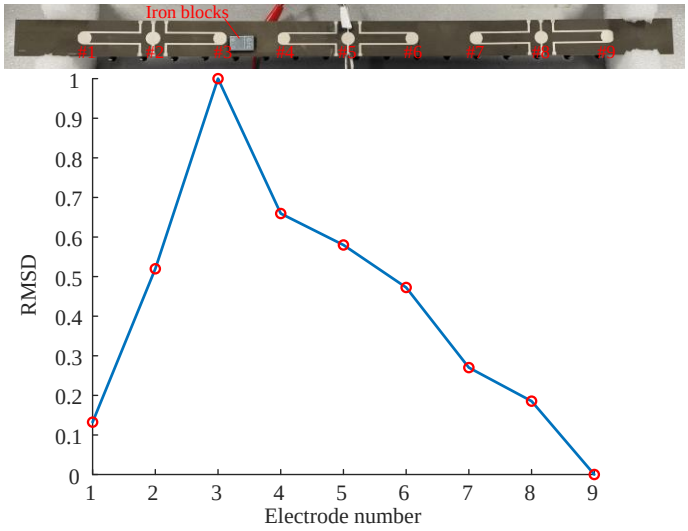

FIGURE 10: RMSD FOR THE DAMAGED CASE

5. CONCLUDING REMARKS AND FUTURE WORK

This paper proposes an intelligent piezoelectric composite structure that utilizes EMIS methodology for establishing structural self-awareness. Coupled-field finite element models were constructed to verify the feasibility of the EMIS for structural active sensing. The manufacturing process of piezoelectric composite structures was introduced in detail, and sample beams were meticulously crafted through a continuous process of material ratio optimization and process step refinement to ensure the highest degree of sensitivity and reliability. Finally, experimental validation of the EMIS method was performed, demonstrating the feasibility and accuracy of the impedance spectra for creating structural self-awareness.

For future work, extending the proposed method to larger-scale structures and more complex damage scenarios should be explored. Further development of the manufacturing process could also improve the efficiency and effectiveness of the proposed approach.

ACKNOWLEDGEMENTS

The support from the National Natural Science Foundation of China (contract numbers 51975357 and 51605284) and the Shanghai Rising-Star Program (contract number 21QA1405100) are thankfully acknowledged. This work was also sponsored by the Wuxi City Huifeng Electronic Co., Limited.

REFERENCES

[1] Jinping Ou and Hui Li, “Structural Health Monitoring in mainland China: Review and Future Trends,” *Struct. Health Monit.*, vol. 9, no. 3, pp. 219–231, May 2010, doi: 10.1177/1475921710365269.

[2] G. Victor, “Structural health monitoring with piezoelectric wafer active sensors – predictive modeling and simulation,” *INCAS Bull.*, vol. 2, no. 3, pp. 31–44, Sep. 2010, doi: 10.13111/2066-8201.2010.2.3.4.

[3] S. Minakuchi and N. Takeda, “Recent advancement in optical fiber sensing for aerospace composite structures,” *Photonic Sens.*, vol. 3, no. 4, pp. 345–354, Dec. 2013, doi: 10.1007/s13320-013-0133-4.

[4] A. V. Krishnamurthy, M. Anjanappa, Z. Wang, and X. Chen, “Sensing of Delaminations in Composite Laminates using Embedded Magnetostrictive Particle Layers,” *J. Intell. Mater. Syst. Struct.*, vol. 10, no. 10, pp. 825–835, Oct. 1999, doi: 10.1106/6UR5-7LE3-QV3H-AG6V.

[5] T. N. Tallman, S. Gungor, K. W. Wang, and C. E. Bakis, “Tactile imaging and distributed strain sensing in highly

flexible carbon nanofiber/polyurethane nanocomposites," *Carbon*, vol. 95, pp. 485–493, Dec. 2015, doi: 10.1016/j.carbon.2015.08.029.

[6] G. J. Gallo and E. T. Thostenson, "Electrical characterization and modeling of carbon nanotube and carbon fiber self-sensing composites for enhanced sensing of microcracks," *Mater. Today Commun.*, vol. 3, pp. 17–26, Jun. 2015, doi: 10.1016/j.mtcomm.2015.01.009.

[7] G. Haghiashtiani and M. A. Greminger, "Fabrication, polarization, and characterization of PVDF matrix composites for integrated structural load sensing," *Smart Mater. Struct.*, vol. 24, no. 4, p. 045038, Apr. 2015, doi: 10.1088/0964-1726/24/4/045038.

[8] Q. Liu, Y. Li, R. Guan, J. Yan, and M. Liu, "Advancing measurement of zero-group-velocity Lamb waves using PVDF-TrFE transducers: first data and application to in situ health monitoring of multilayer bonded structures," *Struct. Health Monit.*, p. 147592172211268, Nov. 2022, doi: 10.1177/14759217221126812.

[9] V. Giurgiutiu and A. Zagrai, "Damage Detection in Simulated Aging-Aircraft Panels Using the Electro-Mechanical Impedance Technique," in *Adaptive Structures and Material Systems*, Orlando, Florida, USA: American Society of Mechanical Engineers, Nov. 2000, pp. 349–358. doi: 10.1115/IMECE2000-1725.

[10] M. Gresil, L. Yu, V. Giurgiutiu, and M. Sutton, "Predictive modeling of electromechanical impedance spectroscopy for composite materials," *Struct. Health Monit.*, vol. 11, no. 6, pp. 671–683, Nov. 2012, doi: 10.1177/1475921712451954.

[11] C. K. Soh, K. K.-H. Tseng, S. Bhalla, and A. Gupta, "Performance of smart piezoceramic patches in health monitoring of a RC bridge," *Smart Mater. Struct.*, vol. 9, no. 4, pp. 533–542, Aug. 2000, doi: 10.1088/0964-1726/9/4/317.

[12] B. Sabet Divsholi and Y. Yang, "Combined embedded and surface-bonded piezoelectric transducers for monitoring of concrete structures," *NDT E Int.*, vol. 65, pp. 28–34, Jul. 2014, doi: 10.1016/j.ndteint.2014.03.009.

[13] H. Kim, X. Liu, E. Ahn, M. Shin, S. W. Shin, and S.-H. Sim, "Performance assessment method for crack repair in concrete using PZT-based electromechanical impedance technique," *NDT E Int.*, vol. 104, pp. 90–97, Jun. 2019, doi: 10.1016/j.ndteint.2019.04.004.

[14] G. Park, H. H. Cudney, and D. J. Inman, "Feasibility of using impedance-based damage assessment for pipeline structures," *Earthq. Eng. Struct. Dyn.*, vol. 30, no. 10, pp. 1463–1474, Oct. 2001, doi: 10.1002/eqe.72.

[15] W. S. Na, "Possibility of detecting wall thickness loss using a PZT based structural health monitoring method for metal based pipeline facilities," *NDT E Int.*, vol. 88, pp. 42–50, Jun. 2017, doi: 10.1016/j.ndteint.2017.03.001.

[16] J. Raju, S. Bhalla, and T. Visalakshi, "Pipeline corrosion assessment using piezo-sensors in reusable non-bonded configuration," *NDT E Int.*, vol. 111, p. 102220, Apr. 2020, doi: 10.1016/j.ndteint.2020.102220.

[17] Venu Gopal Madhav Annamdas and Chee Kiong Soh, "Application of Electromechanical Impedance Technique for Engineering Structures: Review and Future Issues," *J. Intell. Mater. Syst. Struct.*, vol. 21, no. 1, pp. 41–59, Jan. 2010, doi: 10.1177/1045389X09352816.

[18] G. Park, H. Sohn, C. R. Farrar, and D. J. Inman, "Overview of Piezoelectric Impedance-Based Health Monitoring and Path Forward," *Shock Vib. Dig.*, vol. 35, no. 6, pp. 451–463, Nov. 2003, doi: 10.1177/05831024030356001.

[19] V. Giurgiutiu and A. Zagrai, "Damage Detection in Thin Plates and Aerospace Structures with the Electro-Mechanical Impedance Method," *Struct. Health Monit.*, vol. 4, no. 2, pp. 99–118, Jun. 2005, doi: 10.1177/1475921705049752.